



日本原子力研究開発機構機関リポジトリ
Japan Atomic Energy Agency Institutional Repository

Title	Validating polarization effects in γ -rays elastic scattering by Monte Carlo simulation
Author(s)	Omer M., Hajima Ryoichi
Citation	New Journal of Physics,21(11),p.113006_1-113006_10
Text Version	Published Journal Article
URL	https://jopss.jaea.go.jp/search/servlet/search?5067365
DOI	https://doi.org/10.1088/1367-2630/ab4d8a
Right	©2019 The Author(s). Published by IOP Publishing Ltd on behalf of the Institute of Physics and Deutsche Physikalische Gesellschaft

PAPER • OPEN ACCESS

Validating polarization effects in γ -rays elastic scattering by Monte Carlo simulation

To cite this article: Mohamed Omer and Ryoichi Hajima 2019 *New J. Phys.* **21** 113006

View the [article online](#) for updates and enhancements.



PAPER

Validating polarization effects in γ -rays elastic scattering by Monte Carlo simulation

OPEN ACCESS

RECEIVED

20 May 2019

REVISED

16 September 2019

ACCEPTED FOR PUBLICATION

14 October 2019

PUBLISHED

1 November 2019

Original content from this work may be used under the terms of the [Creative Commons Attribution 3.0 licence](#).

Any further distribution of this work must maintain attribution to the author(s) and the title of the work, journal citation and DOI.

Mohamed Omer^{1,3} and Ryoichi Hajima^{1,2} ¹ Integrated Support Center for Nuclear Nonproliferation and Nuclear Security, Japan Atomic Energy Agency, Tokai, Ibaraki, 319-1195 Japan² Tokai Quantum Beam Science Center, National Institutes for Quantum and Radiological Science and Technology, Tokai, Ibaraki 319-1106, Japan³ Permanent address: Physics Department, Assiut University, Assiut, 71516, Egypt.E-mail: omer.mohamed@jaea.go.jp**Keywords:** γ -ray elastic scattering, polarization effects, Monte Carlo simulation, Stokes parameters

Abstract

The polarization properties of γ -rays elastically scattered by atoms have become more observable with the development of polarized photon beams. However, systematic studies are required to explore the elastic scattering in the MeV-energy range of the spectrum where Delbrück scattering becomes more significant, especially at large scattering angles. We implement a new Monte Carlo simulation to account for the polarization effects of elastic scattering. The simulation is based on explicit expressions driven in the formalism of Stokes parameters. The scattering amplitudes of Rayleigh, nuclear Thomson, and Delbrück scattering processes are superimposed onto a two orthogonal set of complex amplitudes. This set is then exploited to construct the core of the simulation in such a way that the simulation can handle arbitrary polarization states of the incoming beam and correspondingly generate polarization states of the outgoing beam. We demonstrate how the polarization of scattered photons is affected by the polarization of incoming photons. In addition, we explain the dependence of depolarization on the azimuthal angle.

1. Introduction

Elastic scattering of γ -rays by atoms comprises four sub-processes, namely, Rayleigh scattering, nuclear Thomson scattering, Delbrück scattering, and nuclear resonance scattering. Of these, Rayleigh scattering and nuclear Thomson scattering are associated with the scattering of a photon by electronic and nuclear charges of an atom, respectively. On the other hand, Delbrück scattering is an interaction between a photon and the strong Coulomb field in the proximity of a nucleus. Nuclear resonance scattering is associated with giant dipole resonance, and its contribution becomes appreciable when the energy of the incident photons exceeds approximately 5 MeV [1]. All sub-processes contribute coherently to the scattering cross section via individual scattering amplitudes. The cross section of elastic scattering is proportional to the square of the resultant scattering amplitudes. Many experimental findings pertaining to the differential cross section have been accounted for based on superposition of the four sub-processes. However, validation of the theoretical calculations against experimental observations has focused on the scattering of unpolarized photons [2].

The availability of high-resolution and high-brightness polarized x-ray and γ -ray beams has facilitated investigation of the polarization effects of elastic scattering of photons in the MeV energy range with unprecedented accuracy. Recently, Blumenhagen *et al* [3] measured the polarization transfer caused by elastic scattering of polarized 0.175 MeV photons scattered off gold atoms. They reported strong depolarization of nearly 100% polarized synchrotron radiation. Their finding suggests that elastic scattering has potential use in polarimetry of high-energy photons. Furthermore, Koga and Hayakawa proposed a unique method to measure Delbrück scattering amplitudes separately by employing linearly polarized γ -rays generated by a laser Compton scattering source [4]. An independent measurement of Delbrück scattering would be the first opportunity to

detect a nonlinear quantum electrodynamics phenomenon connected to vacuum polarization [4, 5]. Besides, the elastic scattering of γ -rays affects the studies of nuclear structure by interfering the electromagnetic transitions of the nucleus [6].

Theoretical calculations have predicted that circularly polarized photons might turn into linearly polarized photons upon Rayleigh scattering [7]. This interesting phenomenon, so-called circular dichroism, involves asymmetry in the scattered photon intensity for different helicities of the incident photon. Other theoretical works have focused on polarization effects in Rayleigh scattering beyond nonrelativistic limits [8, 9]. More recently, Surzhykov *et al* [10] proposed the use of Rayleigh scattering as a polarization-diagnostic tool, supported by the experimental results reported in [3]. Nonetheless, these calculations are limited to low energies, where Delbrück scattering has a minimal effect. Moreover, validation of these calculations at high energies against experimental observations is still questionable.

Monte Carlo simulation is an indispensable tool for studying the polarization effects of elastic scattering of γ -rays because it represents a bridge connecting the theoretical predictions regarding a γ -ray interaction with the experimental procedures required to investigate the phenomenon. In addition, the simulation can account for unavoidable overlapping of other interactions with the elastic scattering such as small angle Compton scattering. Also, the particle transport simulation takes into account the multiple scattering events and polarization mixing at each scattering event. Many simulations have been implemented to account for the elastic scattering of unpolarized photons [11], as well as linearly polarized photons [12, 13]. Other simulations have exploited Stokes parameters formalism to handle different states of polarization [14, 15]. However, the treatment of elastic scattering is limited to an oversimplified approximation of Compton scattering, ignoring the complexity of the interaction.

In the present study, we analyze the elastic scattering phenomenon by using a matrix representation of polarization [16] based on Stokes parameters formalism. This analysis results in a set of direct expressions that highlight the general features of polarization effects in γ -ray elastic scattering. Then, we develop a Monte Carlo simulation based on our analysis by which arbitrary states of polarization of incoming or outgoing photons can be investigated.

2. Theory

Generally, the probability of detecting an elastically scattered γ -ray photon with energy E by an atom of atomic number Z at a scattering angle θ can be expressed as a function of two complex and orthogonal sets of scattering amplitudes, $A_{\parallel}(E, Z, \theta)$ and $A_{\perp}(E, Z, \theta)$, and polarization of the incident and scattered photons. Here, we consider A_{\parallel} to be parallel to the scattering plane (defined by the momentum direction and the electric field vector of the incident photon), while A_{\perp} is perpendicular to the scattering plane. According to the matrix representation of polarization by using Stokes parameters, this probability is given as follows

$$d\sigma = \xi'^T \mathcal{T}_{\text{ES}} \xi, \quad (1)$$

where \mathcal{T}_{ES} is a 4×4 polarization transfer matrix. ξ and ξ' are the normalized Stokes vectors of the incident and scattered beams, respectively.

For zero-target polarization, that is, the target atoms are oriented randomly, the transformation matrix can be simply written for a linear diattenuator because, in general $A_{\parallel} \neq A_{\perp}$. In a coordinate frame in which the incident photon is directed to the positive z -axis, the differential cross section then reads

$$d\sigma = \frac{1}{4} \begin{pmatrix} 1 & \xi'_1 & \xi'_2 & \xi'_3 \end{pmatrix} \times \begin{pmatrix} (|A_{\parallel}|^2 + |A_{\perp}|^2) & (|A_{\parallel}|^2 - |A_{\perp}|^2) & 0 & 0 \\ (|A_{\parallel}|^2 - |A_{\perp}|^2) & (|A_{\parallel}|^2 + |A_{\perp}|^2) & 0 & 0 \\ 0 & 0 & (A_{\parallel}A_{\perp}^* + A_{\parallel}^*A_{\perp}) & i(A_{\parallel}^*A_{\perp} - A_{\parallel}A_{\perp}^*) \\ 0 & 0 & i(A_{\parallel}A_{\perp}^* - A_{\parallel}^*A_{\perp}) & (A_{\parallel}A_{\perp}^* + A_{\parallel}^*A_{\perp}) \end{pmatrix} \times \begin{pmatrix} 1 \\ \xi_1 \\ \xi_2 \\ \xi_3 \end{pmatrix}. \quad (2)$$

In the Stokes parameters notation considered herein, $\xi_1 = +1(-1)$ represents linear polarization with the electric field vector parallel to the x -axis (y -axis). ξ_2 denotes linear polarization in a direction that makes an angle of $\pi/4$ to the right of x -axis. $\xi_3 = +1(-1)$ denotes circular polarization with photon helicity in the clockwise (anti-clockwise) direction.

It should be noted that equation (2) corresponds to equation (11) in [17] and equation (2.1.9) in [18], but the matrix representation provides formulations for the polarization of scattered photons as well as for the dependence of scattered photon polarization on the azimuthal angle. Furthermore, the matrix representation simplifies implementation of the Monte Carlo simulation of the process within a unified and inclusive

framework. The polarization vector of scattered photons can be calculated directly as

$$\xi' = \mathcal{T}_{\text{ES}}\xi. \quad (3)$$

In the following subsections, we analyze the possible effects of the polarization of incident and scattered photons in terms of matrix representation.

2.1. Scattering of unpolarized γ -rays

The Stokes parameters of an unpolarized photon beam are $\xi_1 = \xi_2 = \xi_3 = 0$. This results in a transformation of polarization given by

$$\mathcal{T}_{\text{ES}} \begin{pmatrix} 1 \\ 0 \\ 0 \\ 0 \end{pmatrix} \sim \frac{1}{4} \begin{pmatrix} |A_{\parallel}|^2 + |A_{\perp}|^2 \\ |A_{\parallel}|^2 - |A_{\perp}|^2 \\ 0 \\ 0 \end{pmatrix}.$$

The scattered photon is then linearly polarized with the degree of polarization

$$\xi'_1 = \frac{(|A_{\parallel}|^2 - |A_{\perp}|^2)}{(|A_{\parallel}|^2 + |A_{\perp}|^2)}. \quad (4)$$

If $A_{\perp} \ll A_{\parallel}$, the scattered photon exhibits approximately complete linear polarization in the direction of the scattering plane ($\xi'_1 \approx +1$). The opposite holds as well, that is, if $A_{\parallel} \ll A_{\perp}$, the scattered photon would exhibit a complete linear polarization orthogonal to the scattering plane. The differential cross section of elastic scattering of an unpolarized beam is

$$d\sigma^{\text{unpol}} = \frac{1}{4}[(|A_{\parallel}|^2 + |A_{\perp}|^2) + \xi'_1(|A_{\parallel}|^2 - |A_{\perp}|^2)]. \quad (5)$$

For a polarization-insensitive detector, the unpolarized cross section is obtained by averaging over the directions of polarization of the scattered γ -rays ($\xi'_1 = \pm 1$). Thus, the unpolarized differential cross section is

$$d\sigma^{\text{unpol}} = \frac{1}{2}(|A_{\parallel}|^2 + |A_{\perp}|^2). \quad (6)$$

2.2. Scattering of linearly polarized γ -rays

The linear polarization of an incident photon is delineated by a non-zero value of either ξ_1 or ξ_2 . In an analysis of the scattering of linearly polarized photons, an appropriate rotation must be performed before transformation by the polarization transfer matrix. This rotation implies a transformation of the Stokes vector of the incident photon with respect to a fixed laboratory frame. Such a transformation follows $\xi \rightarrow \mathcal{M}\xi$ where \mathcal{M} is given as follows

$$\mathcal{M} = \begin{pmatrix} 1 & 0 & 0 & 0 \\ 0 & \cos 2\phi & \sin 2\phi & 0 \\ 0 & -\sin 2\phi & \cos 2\phi & 0 \\ 0 & 0 & 0 & 1 \end{pmatrix}, \quad (7)$$

where ϕ is the angle between the electric field vector of the incident photon and the x -axis of the laboratory frame. This rotation has no effect on the circular polarization parameter of the Stokes vector, ξ_3 . The transformation is mandatory for multiple events of photon elastic scattering within the scattering target.

Assuming $d\sigma_{\perp}$ is the cross section of the scattering of a linearly polarized photon associated with the Stokes parameter ξ_1 , one can directly obtain

$$d\sigma_{\perp} = \frac{1}{4}[(|A_{\parallel}|^2 + |A_{\perp}|^2)(1 + \xi_1\xi'_1\cos 2\phi) + (|A_{\parallel}|^2 - |A_{\perp}|^2)(\xi_1\cos 2\phi + \xi'_1) - \xi_1\xi'_2(A_{\parallel}A_{\perp}^* + A_{\parallel}^*A_{\perp})\sin 2\phi - \xi_1\xi'_3 i(A_{\parallel}A_{\perp}^* - A_{\parallel}^*A_{\perp})\sin 2\phi]. \quad (8)$$

Equation (8) explains the intensity asymmetry of the scattered photons in terms of the azimuthal angle. Two main cases can be distinguished easily. The first case is the intensity measured in the scattering plane corresponding to $\phi = 0$. If we consider that the incident photon is completely linearly polarized, the differential cross section parallel to the scattering plane is $d\sigma_{\perp} = d\sigma_{\parallel} = \frac{1}{2}A_{\parallel}$. The second case involves measurement of the scattered photons in a plane orthogonal to the scattering plane where $\phi = \pi/2$ and $d\sigma_{\perp} = d\sigma_{\perp} = \frac{1}{2}A_{\perp}$.

The scattered photons are, in general, elliptically polarized. However, in these two special cases, the scattered photons are linearly polarized. The degree of linear polarization can be calculated using equation (3). For a polarization-insensitive detector the differential cross section is

$$d\sigma_{\perp} = \frac{1}{4} [|A_{\parallel}|^2 + |A_{\perp}|^2 + \xi_1 (|A_{\parallel}|^2 - |A_{\perp}|^2) \cos 2\phi]. \quad (9)$$

Similarly, the cross section of elastic scattering associated with ξ_2 can be expressed as

$$d\sigma_{\gamma} = \frac{1}{4} [(|A_{\parallel}|^2 + |A_{\perp}|^2)(1 + \xi_2 \xi_1' \sin 2\phi) + (|A_{\parallel}|^2 - |A_{\perp}|^2)(\xi_2 \sin 2\phi + \xi_1') \\ + \xi_2 \xi_2' (A_{\parallel} A_{\perp}^* + A_{\parallel}^* A_{\perp}) \cos 2\phi + \xi_2 \xi_3' i (A_{\parallel} A_{\perp}^* - A_{\parallel}^* A_{\perp}) \cos 2\phi]. \quad (10)$$

For polarization-insensitive detectors

$$d\sigma_{\gamma} = \frac{1}{4} [|A_{\parallel}|^2 + |A_{\perp}|^2 + \xi_2 (|A_{\parallel}|^2 - |A_{\perp}|^2) \sin 2\phi] \quad (11)$$

In the case of ξ_2 , the polarization is only preserved at $\phi = \pi/4$ and $\phi = 3\pi/4$ as presumed from equation (10).

2.3. Scattering of circularly polarized γ -rays

The existence of circular polarization in the incident photon, that is $\xi_3 \neq 0$, gives rise to the cross section

$$d\sigma_0 = \frac{1}{4} [|A_{\parallel}|^2 + |A_{\perp}|^2 + \xi_1' (|A_{\parallel}|^2 - |A_{\perp}|^2) \\ + \xi_3 \xi_2' i (A_{\parallel}^* A_{\perp} - A_{\parallel} A_{\perp}^*) + \xi_3 \xi_3' (A_{\parallel} A_{\perp}^* + A_{\parallel}^* A_{\perp})]. \quad (12)$$

Similar to the scattering of linearly polarized photons, the scattering of circularly polarized photons results in elliptically polarized photons. The scattered beam contains a linear polarization component in the scattering plane whenever $A_{\parallel} \neq A_{\perp}$. Additionally, the scattered beam may have a linear polarization component in a plane making an angle of $\pi/4$ with the scattering plane if the term $A_{\parallel}^* A_{\perp} - A_{\parallel} A_{\perp}^*$ is non-zero. Interestingly, Manakove *et al* [7] showed by numerical calculations that circular dichroism may be observed as a result of the Rayleigh scattering of hard x-rays, even with randomly oriented atoms. However, they ignored the correlation between the Stokes vectors of the incident and the scattered beams. This correlation, given by equation (3), does not allow $\xi_2' = 1$ when $\xi_3 = \pm 1$. In the case that the polarization of the scattered photons is not measured, the differential cross section is given by

$$d\sigma_0 = \frac{1}{4} (|A_{\parallel}|^2 + |A_{\perp}|^2). \quad (13)$$

3. Monte Carlo simulation

3.1. Rayleigh scattering amplitudes

Computation of Rayleigh scattering amplitudes follows the method of Kissel *et al* [2, 19]. Wave functions of the self-consistent Dirac-Hartree-Fock-Slater potential were employed to calculate the scattering amplitudes. The scattering amplitudes were expressed in terms of a summation of multipole amplitudes combined with associated Legendre polynomials [20]. The multipole amplitudes give the dependence of the scattering amplitudes on the energy of the scattering photon while the associated Legendre polynomials contains the angular dependence. Depending on the energy of the scattered photons and the shell mutlipoles, 6–60 multipoles were required to converge at four-digits accuracy.

Contributions of K -, L -, and M -shell electrons were considered. Except at the forward angle scattering amplitudes (typically $\theta \leq 10^\circ$), the addition of more shells would have almost no effect on the scattering amplitudes, especially at high energies [10, 17]. At forward angle, the symmetry considerations dictate that $|A_{\parallel}(E, \theta = 0, \pi)| = |A_{\perp}(E, \theta = 0, \pi)|$ which in turn vanishes the Stokes parameter of the scattered photons regardless the scattering amplitudes, as indicated by equation (4). The independence of the scattered photon polarization on the shell contribution beyond M -shell is consistent with the recent calculations made by Surzhykov *et al* [21].

3.2. Delbrück scattering amplitudes

Calculation of Delbrück scattering amplitudes appears to be so difficult to calculate numerically due to convergence problems and singularities in the real and imaginary parts of the amplitude [4, 22, 23]. However, a tabular form of the Delbrück scattering amplitudes calculated in the lowest-order Born approximation is available at wide range of photon energy and scattering angles [24]. This approximation involves proportionality of the scattering amplitude with $(Z\alpha)^2$, where α is the fine structure constant. However, the higher orders include a multi-photon exchange, also known as Coulomb corrections to Delbrück scattering amplitudes. These higher orders result in scattering amplitudes proportional to $(Z\alpha)^{2n}$ with n being the order succeeding the

lowest-order. Corrections, including higher orders, are not considered because the value of the term ($Z\alpha$) decreases rapidly with increasing power [22, 23].

A drawback of the tabulated Delbrück scattering amplitudes is that the scattering amplitudes at forward angle do not exist. We overcame this problem using the analytical formula suggested by Rohrlich and Gluckstern [25]. Then we apply a cubic interpolation on the individual scattering amplitudes. To check the validity of interpolation, we compared the obtained Delbrück amplitudes with those calculated in [1] at photon energy of 2.75 MeV for uranium, lead, tantalum, cerium, and tin. The comparison resulted in a maximum difference of 1.5%. This small difference arises from the fact that Delbrück amplitudes (both dispersive and absorptive parts) have a monotonic trend causing no issues with the interpolation procedure.

3.3. Nuclear Thomson and nuclear scattering amplitudes

The nuclear Thomson scattering amplitudes were calculated assuming that the atomic nucleus can be considered a point charge. This assumption is justified by the fact that the energies of photons considered in the present work are in the MeV range. As a result, the atomic nucleus (of size 10^{-15} m) can safely be considered a point charge. The nuclear Thomson amplitudes are given by (in units of the classical electron radius) $A_{\perp} = -Z^2 m/M$ and $A_{\parallel} = A_{\perp} \cos \theta$, where M is the nuclear mass.

The nuclear resonance scattering amplitudes can be calculated analytically as a low energy tail of the giant dipole resonance. In the present work, we did not include the scattering amplitudes of nuclear resonance scattering owing to their weak effect in the energy region of up to 5 MeV [1].

3.4. Implementing the simulation

Geant4 [26] is a Monte Carlo particle transport framework used to simulate various electromagnetic and hadronic interactions of particles with matter. In Geant4, particle polarization can be handled using the so-called polarization vector, which represents the Stokes polarization vector with the same convention as that mentioned in the previous section. The integrated cross section of the interaction must be introduced into the simulation toolkit such that the sampling of the process, among other competing processes, is calculated based on the integrated cross section. On the other hand, the differential cross sections serve as a probability distribution function of the angular distribution at the exit channel of the interaction. In the present work, we developed a new electromagnetic interaction model to account for polarization effects in γ -ray elastic scattering. The differential cross section of the interaction is calculated using equation (6), where the polarization states of the outgoing photons are calculated using equation (3). The total cross section is computed numerically by using the method described in our recent work [27] and confirmed by others [28].

To handle the azimuthal angular distributions arising from the linear polarization effects, namely, ξ_1 and ξ_2 , we prepared a particular function for sampling the azimuthal angle. In this function, a $\cos^2 \phi$ distribution is generated in terms of $|A_{\parallel}|^2$, $|A_{\perp}|^2$, and the rotation angle of which the polarization plane of the incident beam is making with a fixed laboratory frame. In the case of the second Stokes parameter, an additional phase of $\pi/4$ is implemented according to the definition of the second Stokes parameter. For circular polarization, the polar angle is resampled according to the distribution given by equation (12), while the azimuthal angle is sampled uniformly.

Finally, polarization mixing is realized by using a probability distribution function composed of the three differential cross sections given by equations (8), (10), and (12). However, if the polarization of the scattered photon is not measured, this probability function is calculated using equations (9), (11), and (13). Notably, polarization mixing is important for the multiple scattering events, as well as polarization impurity, encountered in practical situations [3, 10].

4. Results and discussion

In this section, we present examples of our calculations performed by conducting Monte Carlo simulations. The calculation examples were selected carefully to match the existing experimental measurements. Various types of measurements can be found in the literature, and all of them are related to the linear polarization of either the incoming photons, outgoing photons, or both.

4.1. Scattering of unpolarized photons

The first type of measurements is concerned with the linear polarization resulting from the elastic scattering of initially unpolarized photons. The degree of linear polarization of the scattered photons is given by equation (4). Usually, polarization of the scattered photons is determined experimentally by using a Compton polarimeter. Among the early examples of such measurements are the works of Williams and McNeil [29] and Singh and Sood [30]. As shown in figure 1(a), the results of a simulation of the elastic scattering of 1.33 MeV unpolarized

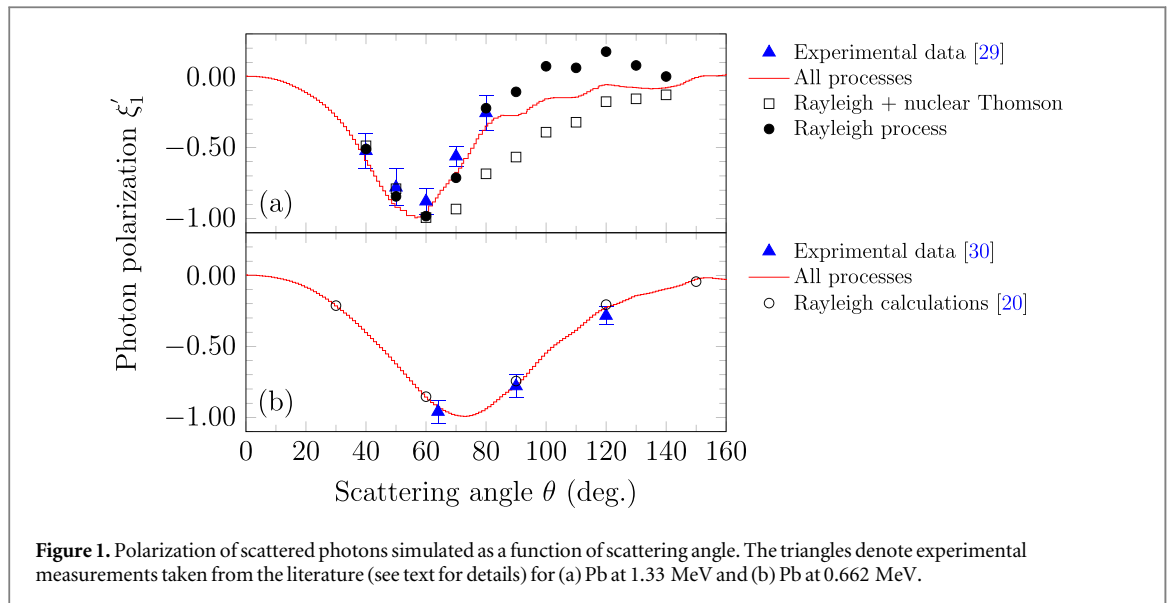


Figure 1. Polarization of scattered photons simulated as a function of scattering angle. The triangles denote experimental measurements taken from the literature (see text for details) for (a) Pb at 1.33 MeV and (b) Pb at 0.662 MeV.

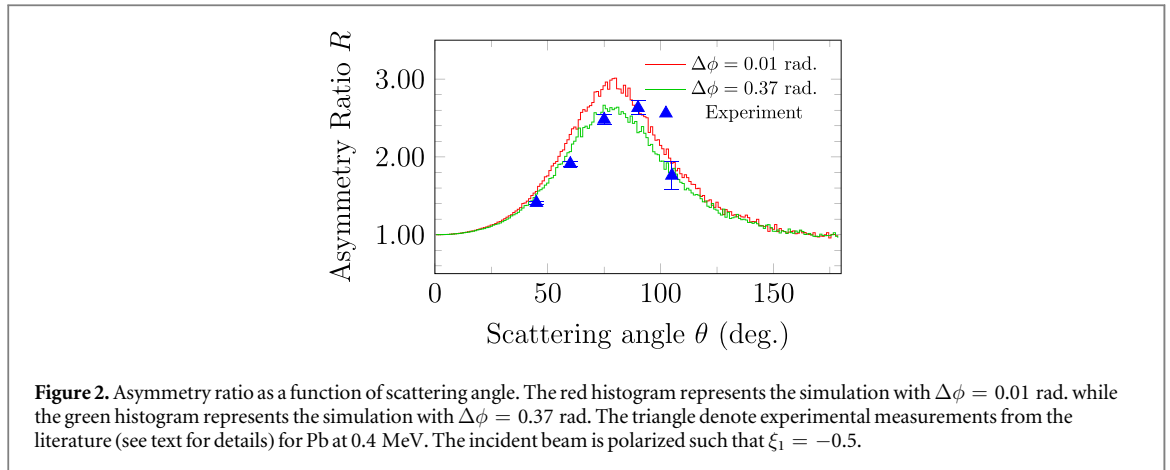
photons by lead agree well with the experimental data in [29]. Similarly, the results of the simulation of 0.662 MeV photons agree well with the data in [30] as shown in figure 1(b). Notably, an interference pattern is observed in the simulation at higher energies. This pattern originates from the interference of multipole amplitudes, which are summed with factors of varying signs at large angles when summed up to compose the total-atom Rayleigh scattering amplitudes. Also, the magnitudes of the amplitudes are very small compared to the small angle amplitudes. This gives rise to an increase in the error of the calculations [2].

Unlike the predictions made using the theory of form factor approximation, the geometrical maxima of the polarization of scattered photons deviate from 90° as the energy of the photons increase. This is because the form factor approximation is independent of the polarization of the incident photons. Furthermore, the deviation of the geometrical maxima increases with heavy scatterers because the Delbrück scattering amplitudes become more effective.

The Stokes parameter, ξ'_1 shown in figure 1 indicates a remarkable feature that the polarization plane of the scattered photon is orthogonal to the scattering plane. This is identical to the effect of Compton scattering. However, there are favorable cases in which the polarization of the scattered photons is parallel to the scattering plane. The former case corresponds to $A_{\parallel} \geq A_{\perp}$ while the latter corresponds to $A_{\perp} \geq A_{\parallel}$. It can be inferred from figure 1 that the magnitude of polarization due to the elastic scattering approaches unity at 56° for the 1.33 MeV photons and at 73° for the 0.662 MeV-photons. This magnitude cannot be attained by Compton scattering of unpolarized beams (maximum degrees of polarization are 40% and 61% at 1.33 and 0.662 MeV, respectively). Therefore, despite the fact Compton scattering has a larger cross section than elastic scattering, the elastic scattering of γ -rays acts as a perfect polarizer for high energy γ -rays with the advantage of preserving the photon energy.

A comparison between our simulation and calculations performed by Johnson and Cheng [20] is shown in figure 1(b). The simulation data set for the scattering of 0.662 MeV photons off lead atoms agrees with the calculations provided in [20]. At this energy, Rayleigh scattering amplitudes dominate those of nuclear Thomson and Delbrück processes, especially at small angles. For example, ξ'_1 at 30° increases only by approximately 0.6% (0.7%) when including nuclear Thomson (Delbrück) amplitudes. However, at large angles, for example, 120° the polarization of the scattered photon change from $\xi'_1 = -0.206$ to $\xi'_1 = -0.245$ with a change of 19% upon adding nuclear Thomson amplitude. Moreover, the polarization of the scattered photon reaches $\xi'_1 = -0.229$ with a change of 11% upon adding Delbrück amplitudes. The significance of nuclear Thomson and Delbrück amplitudes appears at large angle scattering because Rayleigh amplitudes fall more rapidly than nuclear Thomson and Delbrück amplitudes with increasing the scattering angle.

Nuclear Thomson and Delbrück amplitudes gain more importance at higher photon energies. Figure 1(a) demonstrates how each scattering process affects the polarization of the scattered photons whose energy is 1.33 MeV scattered by lead. At forward angles, the effect of nuclear Thomson and Delbrück amplitudes is minimal with respect to pure Rayleigh amplitudes. However, at 120° , the inclusion of Delbrück amplitudes reduces the polarization of the scattered photon by a factor of 3. Despite the lack of experimental measurements of polarization at this energy and scattering angle, the role of Delbrück amplitudes at 1.33 MeV is consistent with measurements of the differential cross section of elastic scattering of 1.33 MeV by uranium provided by Muckenheim and Schumacher [31]. In general, the elastic scattering of photons is a phase-dependent process,



which means the contributing amplitudes must be added coherently before squaring. At forward angles, Rayleigh and nuclear Thomson have the same phase which opposes the phase of Delbrück amplitudes. In contrast, at backward angles, Delbrück amplitudes are in phase with both Rayleigh and nuclear Thomson amplitudes. Depending on the magnitude of Delbrück amplitudes, Delbrück and nuclear Thomson processes tend to cancel each other at forward angles leaving Rayleigh scattering to be the effective process.

4.2. Scattering of partially polarized photons

Many experiments have been performed to study the polarization effects of the elastic scattering of γ -rays [32–34]. In these experiments, the partially polarized incoming beam was generated by Compton scattering of unpolarized γ -rays from radioactive sources. Then, the polarized beam was allowed to hit the elastic scattering targets. Owing to Compton scattering, the incident photons were orthogonally polarized with respect to the scattering plane. Therefore, ξ_1 was generally negative. Such experiments involved measurement of the asymmetry ratio R , which is defined as the ratio of the intensities of the scattered photons in the scattering plane and the scattered photons in a perpendicular plane. Using equation (9), R can be expressed as

$$R = \frac{(|A_{\parallel}|^2 + |A_{\perp}|^2) + \xi_1(|A_{\parallel}|^2 - |A_{\perp}|^2)}{(|A_{\parallel}|^2 + |A_{\perp}|^2) - \xi_1(|A_{\parallel}|^2 - |A_{\perp}|^2)}. \quad (14)$$

In general, the experimentally determined ratios are systematically lower than the theoretically calculated values [17]. This underestimation of R can be interpreted in terms of the depolarization occurring because of the extended detector size over the azimuthal angle. To investigate the dependence of R , we simulated the scattering of a polarized beam with the azimuthal angle extending over $\Delta\phi = 0.01$ and $\Delta\phi = 0.37$ rad. The first case of $\Delta\phi$ corresponds to ideal case in which the size of the detector is negligible. The second case corresponds to the extended detector size defined in the experiment [32].

As shown in figure 2, the measured asymmetry ratios are approximately 20% lower than the expected values. However, the agreement of the measured values is much better if depolarization due to the extended azimuthal angle is considered. The sensitivity of the asymmetry ratio to the extended azimuthal angle can be inferred from figure 3 as well. This figure shows the results of a simulation with 10^9 photons of energy $E = 0.4$ MeV and polarization $\xi_1 = -0.5$ scattered by a lead target. The photons scattered at azimuthal angle of $\phi = 0$ and $\phi = \pi/2$ rad were recorded with angular divergences of $\Delta\phi = 0.01$ and $\Delta\phi = 0.37$ rad. The depolarization caused by extension of the azimuthal angle tended to decrease the numerator of equation (14) to a greater extent than it decreased the denominator. As a result, a small reduction in the asymmetry ratio occurred.

4.3. Polarization transfer

Testing polarization transfer requires one to measure the polarization of the scattered photons when the incident photon is polarized. Recently, an experiment was conducted using approximately completely linearly polarized (degree of linear polarization is 98.01%) synchrotron radiation [3]. The polarization of the scattered photons was measured at three different angles for photons of energy 0.175 MeV scattered by gold. The experimental results indicated that the polarization of the scattered photon exhibited a resonance-like shape with the scattering angle. Moreover, the polarization of the scattered photons was extremely sensitive to the polarization of the incident photon. This sensitivity was found to depend on the relative values of $|A_{\parallel}|^2$ and $|A_{\perp}|^2$.

We benchmarked the proposed method described in the previous section by simulating the elastic scattering of polarized 0.175 MeV photons by gold atoms. The angular distribution of the scattered photons' polarization is shown in figure 4 along with the experimental findings from [3]. Our simulation agrees, within the

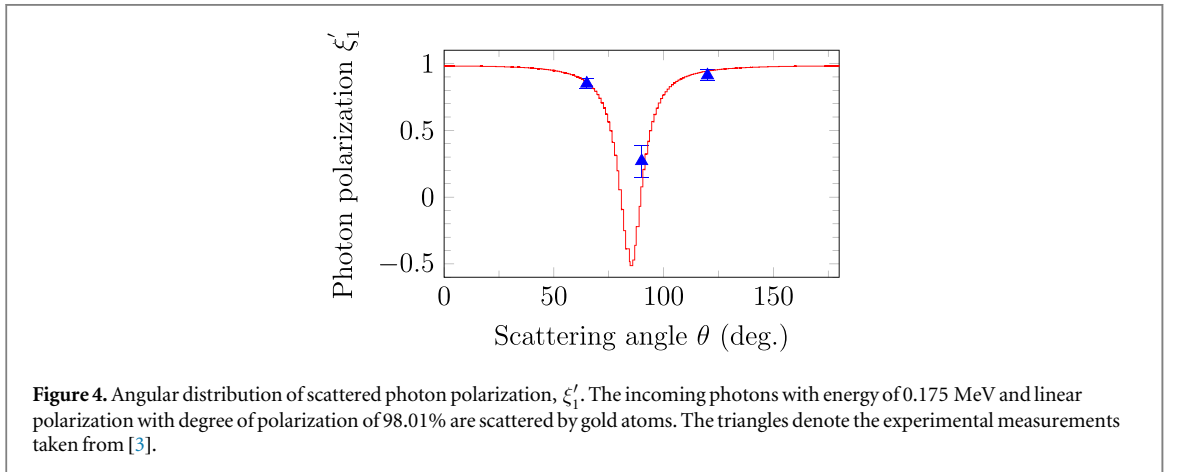
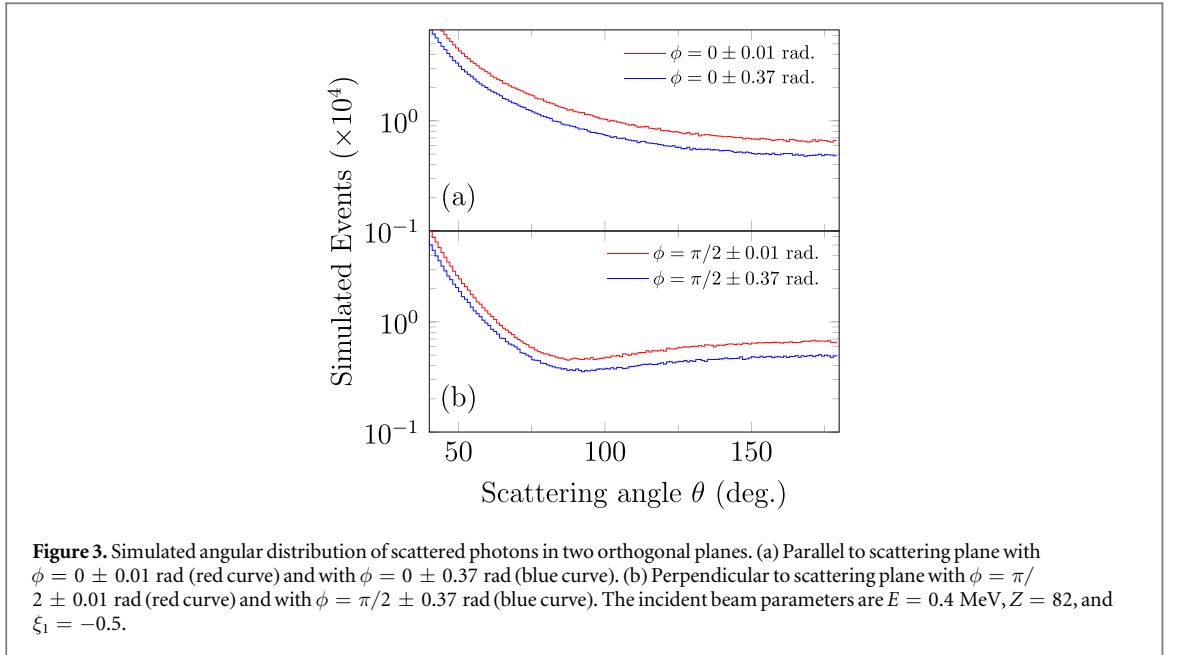


Table 1. Correlation of the Stokes parameter of the incoming beam and scattered beam.

Z	E (MeV)	θ (deg.)	ξ_1 (%)	ξ'_1	
				Previous works	This work
79	0.175	65	98.0	$+85.0 \pm 3.6^a$	+85.9
		90	98.0	$+27.0 \pm 12^a$	+20.7
		120	98.0	$+91.2 \pm 4.2^a$	+94.5
82	0.145	86	90.0	-89.2^b	-89.7
			99.0	-26.1^b	-26.2
			99.9	$+71.8^b$	+71.2

^a Experimental data are from [3].

^b Calculations are from [10].

experimental uncertainty, with the most recently reported experimental results on polarization transfer. We additionally depict numerical values of the polarization of the scattered photons in table 1. Note that if the incident photon is completely polarized, that is, $\xi_1 = +1$, the scattered photons are completely polarized with

$\xi_1' = +1$. By contrast, only 2% reduction in the degree of polarization of the incident photon reduced the degree of polarization of the scattered photons by 27% at 90° .

The results of our simulation are consistent with a recent set of calculations pertaining to Rayleigh scattering by lead [10]. Table 1 shows the polarization of scattered photons for a lead target at an energy of 0.145 MeV and a scattering angle of 86° , which corresponds to the maximum polarization. Here, the effect of the incident photon polarization is more apparent than that in the case of gold. The asymmetry ratio in the case of lead is one order of magnitude higher than that in the case of gold.

It should be emphasized that polarization transfer due to the elastic scattering of γ -rays is strongly correlated to the polarization of the incident beam. This fact is proved experimentally for linear polarization in [3], theoretically in [10], and confirmed in the present work. Similar behavior is also expected for the case of circular polarization. Thus, the circular dichroism effect pointed out in [7], and in the references therein, must be re-investigated considering the correlation between the Stokes vectors of the incoming and outgoing beams. In [7], it was particularly supposed that a complete linear polarization would result from the scattering of a circularly polarized beam. However, our calculations show that the degree of linear polarization of the scattered photons is proportional to $A_{\parallel}^* A_{\perp} - A_{\parallel} A_{\perp}^*$, which is very small especially when Delbrück scattering is not considered. Moreover, the results shown in [7] for uranium at high energy ignored the effect of Delbrück scattering, which is proven experimentally. The present simulation tool may help with a broad exploration of the polarization effects including the circular dichroism phenomenon.

5. Conclusions

To summarize, we analyzed the problem of elastic scattering of γ -rays by using the matrix representation of polarization and Stokes parameters formalism. Explicit formulas of differential cross sections corresponding to the three components of the Stokes vector of the input channel were obtained. We used the Stokes parameter formalism to implement a Monte Carlo simulation tool that considered the polarization effects arising from the elastic scattering of γ -rays. We validated the proposed method by using available experimental data. In particular, three aspects were investigated, including the polarization due to the scattering process, depolarization over the azimuthal angle, and sensitivity of the scattered photon polarization to the incident photon polarization. The implemented simulation can be used to study interesting polarization effects of elastic scattering interaction, especially the circular dichroism associated with linear and circular polarization scenarios, as well as the potential use of elastic scattering as a polarization-diagnostic tool.

Acknowledgments

This work was a part of a study of the nuclear resonance fluorescence aiming at nuclear security and safeguards applications [35], being supported by the subsidiary for ‘promotion of strengthening nuclear security or the like’ of the Ministry of Education, Culture, Sports, Science, and Technology (MEXT), Japan. The authors would like to thank T Shizuma, T Hayakawa, and J Koga for valuable discussions.

ORCID iDs

Mohamed Omer  <https://orcid.org/0000-0001-9668-7545>

Ryoichi Hajima  <https://orcid.org/0000-0002-0383-9851>

References

- [1] Kasten B, Schaupp D, Rullhusen P, Smend F, Schumacher M and Kissel L 1986 *Phys. Rev. C* **33** 1606–15
- [2] Kissel L, Pratt R H and Roy S C 1980 *Phys. Rev. A* **22** 1970–2004
- [3] Blumenhagen K H *et al* 2016 *New J. Phys.* **18** 103034
- [4] Koga J K and Hayakawa T 2017 *Phys. Rev. Lett.* **118** 204801
- [5] Rullhusen P, Mückenheim W, Smend F, Schumacher M, Berg G P A, Mork K and Kissel L 1981 *Phys. Rev. C* **23** 1375–83
- [6] Kahane S, Moreh R and Shahal O 1983 *Phys. Rev. C* **28** 1519–26
- [7] Manakov N L, Meremianin A V, Carney J P J and Pratt R H 2000 *Phys. Rev. A* **61** 032711
- [8] Safari L, Amaro P, Fritzsche S, Santos J P, Tashenov S and Fratini F 2012 *Phys. Rev. A* **86** 043405
- [9] Peshkov A A, Volotka A V, Surzhykov A and Fritzsche S 2018 *Phys. Rev. A* **97** 023802
- [10] Surzhykov A, Yerokhin V A, Fritzsche S and Volotka A V 2018 *Phys. Rev. A* **98** 053403
- [11] Fernández J E 1991 *Phys. Rev. A* **44** 4232–48
- [12] Namito Y, Ban S and Hirayama H 1993 *Nucl. Instrum. Methods Phys. Res. A* **332** 277–83
- [13] Mizuno T, Kamae T, Ng J, Tajima H, Mitchell J, Streitmatter R, Fernholz R, Groth E and Fukazawa Y 2005 *Nucl. Instrum. Methods Phys. Res. A* **540** 158–68

- [14] Fernández J, Hubbell J, Hanson A and Spencer L 1993 *Radiat. Phys. Chem.* **41** 579–630
- [15] Depaola G 2003 *Nucl. Instrum. Methods Phys. Res. A* **512** 619–30
- [16] McMaster W H 1961 *Rev. Mod. Phys.* **33** 8–28
- [17] Roy S C, Sarkar B, Kissel L D and Pratt R H 1986 *Phys. Rev. A* **34** 1178–87
- [18] Kane P, Kissel L, Pratt R and Roy S 1986 *Phys. Rep.* **140** 75–159
- [19] Kissel L 2000 *Radiat. Phys. Chem.* **59** 185–200
- [20] Johnson W R and Cheng K T 1976 *Phys. Rev. A* **13** 692–8
- [21] Surzhykov A, Yerokhin V A, Stöhlker T and Fritzsche S 2015 *J. Phys. B: At. Mol. Opt. Phys.* **48** 144015
- [22] Papatzacos P and Mork K 1975 *Phys. Rep.* **21** 81–118
- [23] Papatzacos P and Mork K 1975 *Phys. Rev. D* **12** 206–18
- [24] Falkenberg H, Hüniger A, Rullhusen P, Schumacher M, Milstein A and Mork K 1992 *At. Data Nucl. Data Tables* **50** 1–27
- [25] Rohrlich F and Gluckstern R L 1952 *Phys. Rev.* **86** 1–9
- [26] Agostinelli S *et al* 2003 *Nucl. Instrum. Methods Phys. Res. A* **506** 250–303
- [27] Omer M and Hajima R 2017 *Nucl. Instrum. Methods Phys. Res. B* **405** 43–9
- [28] Turturica G, Iancu V, Suliman G and Ur C 2018 *Nucl. Instrum. Methods Phys. Res. B* **436** 68–73
- [29] Williams R A and McNeill K G 1965 *Can. J. Phys.* **43** 1078–87
- [30] Singh M and Sood B 1965 *Nucl. Phys.* **64** 502–12
- [31] Muckenheim W and Schumacher M 1980 *J. Phys. G: Nucl. Phys.* **6** 1237–50
- [32] Somayajulu D R S and Lakshminarayana V 1968 *J. Phys. A: Gen. Phys.* **1** 228–35
- [33] Brini D, Fuschini E, Peli L and Veronesi P 1958 *Il Nuovo Cimento (1955–1965)* **7** 877–90
- [34] Brini D, Fuschini E, Murty D S R and Veronesi P 1959 *Il Nuovo Cimento (1955–1965)* **11** 533–45
- [35] Hajima R *et al* 2014 *Eur. Phys. J. Spec. Top.* **223** 1229–36